

# A Low-Wavelength Host Absorption Edge of Cesium-Lithium Borate CsLiB<sub>6</sub>O<sub>10</sub>

© I.N. Ogorodnikov

Ural Federal University after the first President of Russia B.N. Yeltsin,  
620002 Yekaterinburg, Russia

e-mail: i.n.ogorodnikov@urfu.ru

Received August 10, 2022

Revised October 11, 2022

Accepted October 22, 2022

We have carried out an experimental study of the VUV edge of the optical host absorption of cesium-lithium borate crystals CsLiB<sub>6</sub>O<sub>10</sub> (CLBO). The transmission ( $T = 293$  K) and absorption ( $T = 80, 293$  K) spectra were studied, the short-wavelength edge of the transparency band (cutoff wavelength) and the energy position of the edge fundamental absorption at which the absorption coefficient  $k = 50 \text{ cm}^{-1}$  were determined. The absorption edge temperature shift coefficient  $-5.5 \cdot 10^{-4} \text{ eV/K}$  was determined. Based on low-temperature reflection spectra ( $T = 10$  K,  $\theta = 17^\circ$ ,  $E = 7-30$  eV) the Kramers–Kronig method was used to calculate the spectra of optical constants: refractive index ( $n$ ) and absorption index ( $k$ ), real ( $\epsilon_1$ ) and imaginary ( $\epsilon_2$ ) parts of the complex permittivity, as well as the absorption coefficient  $\mu$ . The lowest energy peak, due to electronic transitions from the top of the valence band to the states of the bottom of the conduction band, was studied in the  $\epsilon_2(E)$  spectrum, the thresholds for interband transitions were determined  $E_g = 7.95$  eV. The origin of the fundamental absorption edge of cesium-lithium borate is discussed.

**Keywords:** Cesium-lithium borate CsLiB<sub>6</sub>O<sub>10</sub> (CLBO), host absorption edge, optical properties.

DOI: 10.21883/EOS.2022.12.55250.4011-22

## 1. Introduction

Wide-band borate crystals of alkaline and alkaline-earth metals are of practical interest from the point of view of generation and conversion of coherent ultraviolet (UV) radiation in solid-state systems of short-wave laser technology and integrated optics [1–3]. They are distinguished by a combination of high radiation-optical stability and good nonlinear characteristics. The most well-known crystals of this group include barium beta-borate  $\beta$ -BaB<sub>2</sub>O<sub>4</sub> (BBO) [4,5] and lithium triborate LiB<sub>3</sub>O<sub>5</sub> (LBO) [6], which are widely used to generate the second and third harmonics of YAG laser radiation: Nd or Al<sub>2</sub>O<sub>3</sub>:Ti, for the construction of parametric oscillators and integrated optical waveguides. However, due to fundamental crystal-physical limitations, despite the wide transparency range up to 6–7 eV, these crystals are practically unsuitable for generating higher harmonics [7–10]. To overcome this disadvantage, an analog of LBO — cesium-lithium borate CsLiB<sub>6</sub>O<sub>10</sub> (CLBO) has been developed and synthesized, characterized by purposeful distortion of the crystal lattice achieved by replacing half of lithium atoms in the LBO unit cell with cesium atoms having a larger ionic radius [11–13]. The CLBO crystal proved to be effective precisely for generating the fourth (266 nm) and fifth (213 nm) harmonics of powerful picosecond lasers. High conversion efficiency, a wide spectral operating range and the ability to work with powerful laser radiation (up to 26 GW·cm<sup>-2</sup> [12]) are the reasons for the rapid advancement of this crystal in the field of modern laser technologies.

CLBO crystals are colorless, have a transparency range of 180–2750 nm, belong to the tetragonal spatial symmetry group  $I4_2d$ ; an elementary cell with parameters  $a = 1049.4(1)$  pm,  $c = 893.9(2)$  pm; contains 4 formula units (72 atoms) [14,15]. Despite the differences in the symmetry of the crystal lattice of LBO, CLBO and CsB<sub>3</sub>O<sub>5</sub> (CBO), the boroxigen framework in each of these crystals is formed by anionic groups [B<sub>3</sub>O<sub>7</sub>]<sup>5-</sup>, consisting of similar structural units based on three- and four coordinated boron atoms [16].

The electronic structure of LBO is formed mainly by boroxigen anionic groups with an insignificant contribution of lithium cations [17–22]. A diametrically opposite situation is observed in borate crystals with relatively heavy cations: barium ions in BBO [4,23] and cesium in CBO [21,24] make a noticeable contribution to the formation of the electronic structure of these crystals. It is known [25] that the partial composition of the states of the vertex of the valence band (VB) and the bottom of the conduction band (CB), which cause the lowest-energy electronic transitions and the nature of the edge of the fundamental absorption of the crystal, is decisive for many practical applications of optical material. Previously, these issues were studied in detail in relation to BBO [26] and LBO [27] crystals.

In this respect, CLBO crystals occupy an intermediate position between lithium and cesium borates, so the question of the contribution of lithium and cesium ion states to the electronic structure of CLBO and, in particular, to the formation of states determining the nature of the long-wave

edge of the fundamental absorption of CLBO located in the vacuum ultraviolet (VUV) region remains debatable.

The aim of this work is an experimental study of the VUV edge of the fundamental optical absorption of CLBO crystals, obtaining quantitative characteristics by optical VUV spectroscopy methods, including calculations of optical constants based on low-temperature ( $T = 10$  K) reflection spectra measured in a wide range of photon energies 7–32 eV.

## 2. Research targets and methods

In this work, unalloyed (nominally pure) single crystals of optical quality CLBO grown at the Institute of Geology and Mineralogy SB RAS (Novosibirsk) by the Chokhralsky method from stoichiometric composition under conditions of high temperature gradient up to 30 K/cm [28] were used. As a result of optimization of growing regimes, crystals without cracks, inclusions visible under tenfold magnification were obtained. For spectroscopic studies, samples with dimensions of  $8 \times 8 \times 1$  mm with polished plane-parallel surfaces perpendicular to the crystallographic axis  $C$  were used.

Optical measurements were carried out on an experimental setup including a vacuum monochromator VMR-2 with a spherical lattice 600 lines/mm, a high-power monochromator MDR-2 with a lattice 1200 lines/mm; photoelectronic multipliers FEU-106 and FEU-142 operating in the photon counting regime; a hydrogen lamp VMF-25 as a source of optical radiation in the field of vacuum ultraviolet; a vacuum optical chamber with windows made of  $MgF_2$ , equipped with a low-inertia cryostat with replaceable nodes for operation in a wide temperature range from  $T = 10$  to 600 K, and oil-free pumping means. Spectra of optical transmission ( $T$ ) and optical absorption ( $k$ ) are obtained using the following relations:

$$T(E) = \frac{I(E)}{I_0}; \quad k(E) = -\frac{1}{d} \ln(T), \quad (1)$$

where  $I_0$  is intensity of the incident beam;  $I(E)$  is intensity of the transmitted beam;  $E$  is photon energy;  $d$  is sample thickness in centimeters. The optical transmission  $T$  is represented as a percentage, the optical absorption coefficient  $k$  is represented in inverse centimeters.

Low-temperature reflection spectra ( $T = 10$  K,  $\theta = 17^\circ$ ,  $E = 4$ –33 eV) were measured in our early work [29] and presented in it without reference to absolute values of the reflection coefficient. The article [29] gives all the necessary details of the experiment, we only note that the primary monochromator with a platinum-coated diffraction grating provided a spectral resolution of 0.32 nm in the energy range 4–40 eV. In this article, reference was made to the absolute values of the reflection coefficient by the Fresnel relations based on the known dispersion of the refraction indices of LTB and LBO in the visible region of the spectrum [14,30].

## 3. Experimental results

### 3.1. Transmission and absorption spectra

Fig. 1 shows fragments of the optical transmission and absorption spectra of the CLBO measured in the VUV region of the edge of the fundamental absorption of the crystal at room temperature without correction for reflection. In the long-wavelength region, the transmission spectrum (Fig. 1, *a*) is represented by a smooth almost horizontal line without any dips, in the short-wavelength region of the spectrum there is a sharp decrease in crystal transparency to almost zero. The characteristic wavelength separating these two spectral regions is called the cutoff wavelength  $\lambda_c$  and is defined as follows: the transmission spectrum  $T(\lambda)$  in the region of a sharp decrease in transparency is approximated by a straight line, extrapolation of which to the intersection with the abscissa axis gives the value  $\lambda = \lambda_c$ . For the CLBO crystal, the short-wave boundary of the optical transparency band is characterized by a threshold cutoff wavelength  $\lambda_c = 180$  nm (Fig. 1, *a*), which is consistent with the data of earlier works [11,13].

To discuss the absorption spectrum, two characteristic energy points  $E_1$  and  $E_2$  were used, in which the optical absorption is 3 and  $50 \text{ cm}^{-1}$ , respectively (Fig. 1, *b*). In the optical transparency region of CLBO at  $E < E_1 = 6.74$  eV no optical absorption bands were detected. At the energies above  $E_1$ , a monotonous exponential increase in optical absorption is observed, due to the fundamental absorption of the crystal, for example, at the energy  $E_2 = 6.91$  eV the value of the absorption coefficient reaches  $k = 50 \text{ cm}^{-1}$ . The value of  $E_2$  can be taken as the energy position of the long-wave edge of the optical absorption of CLBO in the VUV region of the spectrum. We note that the cutoff wavelength  $\lambda_c$  formally corresponds to the energy  $6.89 \text{ eV} < E_2$ .

### 3.2. Spectra of optical constants

The reflection spectra of the CLBO crystal were measured in a wide energy range of 7–32 eV at  $T = 9.3$  and 293 K. We note two important circumstances. Firstly, due to the qualitative similarity of these spectra, only the low-temperature reflection spectrum ( $T = 9.3$  K) is discussed further, and the second of them ( $T = 293$  K), which turned out to be qualitatively similar to the first, but shifted to the low-energy region ( $\Delta E = -0.155$  eV in the vicinity of the absorption edge), was used only to estimate the temperature shift of the edge of the fundamental absorption (table). Secondly, in order to bind to the absolute values of the reflection coefficient, the experimental spectra (7–30 eV) were compared with the low-energy reflection spectrum (4–7 eV) calculated on the basis of the known dispersion of the refractive indices of CLBO in the crystal transparency region [14,30].

Fig. 2, *a* shows the calibrated reflection spectrum  $R(E)$  of a CLBO crystal for the energy range 7–30 eV. Attention

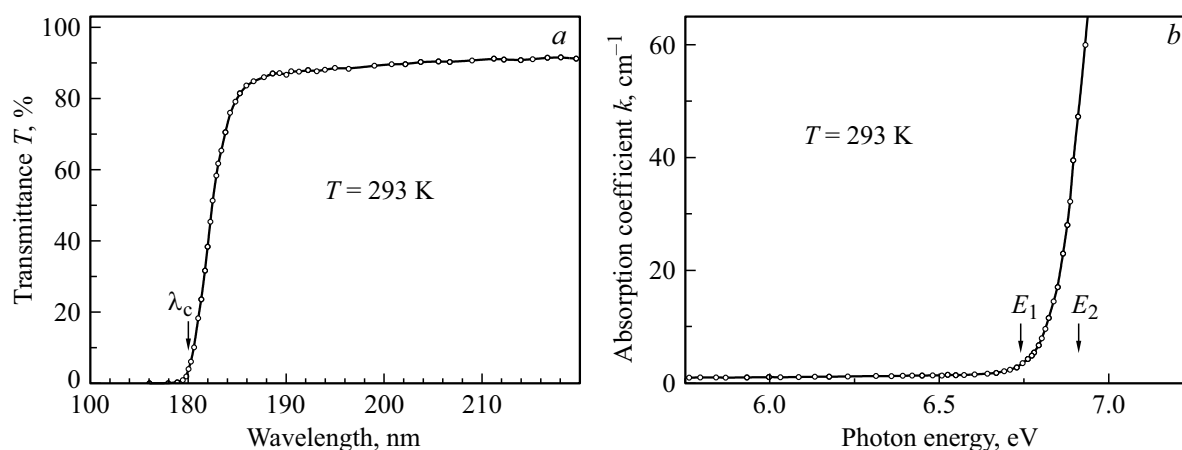


**Figure 1.** Optical transmission spectra (a) and absorption (b) of the LBO measured in the VUV region of the edge of the fundamental absorption of the crystal.

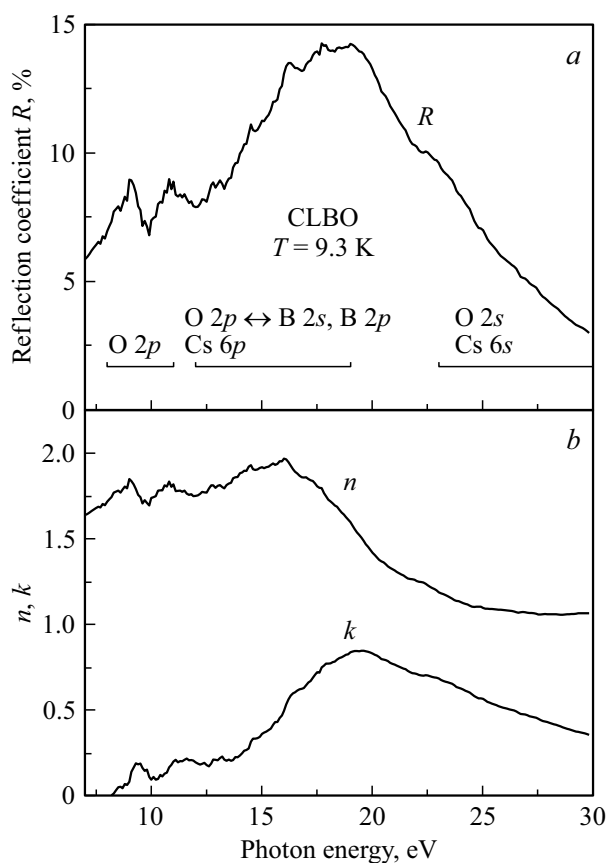


**Figure 2.** Low-temperature reflection spectra ( $R$ ) of a CLBO crystal ( $T = 9.3\text{ K}$ ,  $\theta = 17^\circ$ ) (a); the design base spectra of optical functions  $n$  and  $k$ , obtained by processing  $R(E)$  using the Kramers–Kronig method (b).

is drawn to the relatively small value of the reflection coefficient, the absence of sharp intense peaks characteristic of the exciton structure of the reflection spectra. When the photon energy changes from the transparency region, the

reflection coefficient monotonically increases, the „shoulder“ is observed above the absorption edge at 8.45 eV and two local maxima of equal intensity at 9.0 and 10.8 eV. In the studied energy range, the absolute maximum of the reflection coefficient is reached in the energy range of 17.7–19.0 eV. Further, when the energy changes to 30 eV, a smooth monotonous decline in the reflection coefficient occurs.

Based on the experimental reflection spectrum (Fig. 2, a), we have calculated the spectra of CLBO optical constants using the difference method of Kramers-Kronig integral relations, the description of which is given in the classical work [31]. In the calculation process, the phase correction of the reflection coefficient was carried out, the theoretical principles of which are formulated in the fundamental work [25].

Fig. 2 shows the design base spectra of optical functions  $n$  (refractive index) and  $k$  (absorption index) obtained by processing low-temperature reflection spectra  $R(E)$  using the Kramers–Kronig method. From Fig. 2, b it can be seen that in the spectrum of  $n(E)$  the low-energy maximum is located at 9.0 eV, followed by a minimum at 9.6–9.8 eV, the second maximum at 10.6–10.7 eV and a weakly structured region 12.0–16.0 eV, in which the refractive index reaches a maximum value of  $n = 1.9$ . In the region of 16–30 eV, there is a smooth monotonous decline of the refractive index to the value of  $n = 1.05$ . A detailed examination also revealed the presence of a low-intensity arm in the region of 8.3 eV.

The spectrum of  $k(E)$  in the energy range of 7–19 eV is characterized by a shoulder at 8.4–8.6 eV, two local maxima at 9.4–9.5 and 11.2–11.6 eV, as well as the main broad maximum at 19.2–19.6 eV. In the region of 20–30 eV, there is a smooth monotonous decline in the absorption index.

Based on the obtained optical functions  $n(E)$  and  $k(E)$ , other optical functions were calculated: real ( $\epsilon_1$ ) and imaginary ( $\epsilon_2$ ) components of the complex permittivity

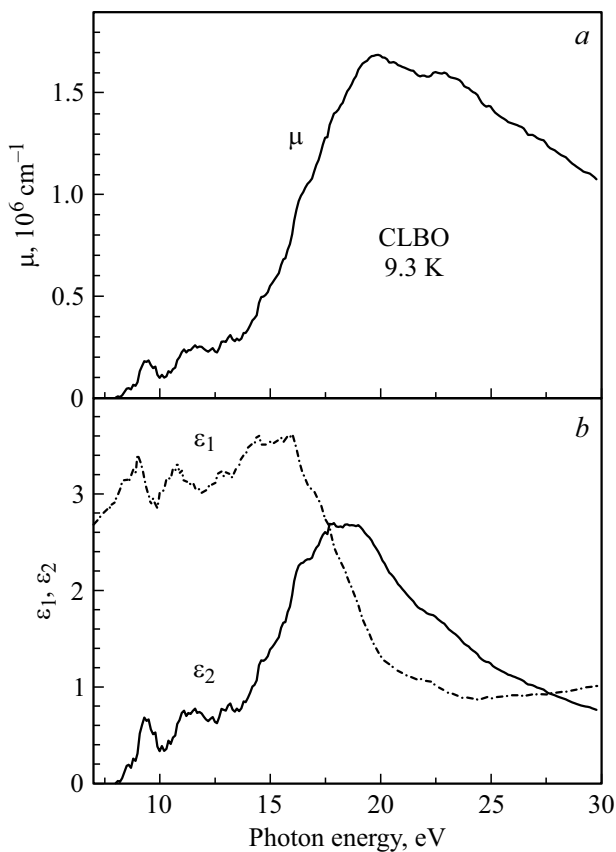


**Figure 3.** The design base spectra of optical functions  $\mu$  (a);  $\varepsilon_1$  and  $\varepsilon_2$  (it b) obtained by processing  $R(E)$  by the Kramers–Kronig method.

$\varepsilon = \varepsilon_1 + i\varepsilon_2$ , as well as the absorption coefficient  $\mu(E)$ :

$$\begin{aligned} \mu &= 4\pi k/\lambda; \\ \varepsilon_1 &= n^2 - k^2; \\ \varepsilon_2 &= 2nk, \end{aligned} \quad (2)$$

where  $\lambda$  —the incident light wavelength, cm.

The absorption spectrum of  $\mu(E)$  (Fig. 3, a) in the region 7–14.0 eV demonstrates a curve whose structural features correspond to those for  $k(E)$ , and the value of the absorption coefficient does not exceed  $3 \cdot 10^5 \text{ cm}^{-1}$ . With a further increase in energy, a steeply increasing curve  $\mu(E)$  is observed, which in the region of 19.5–20.0 eV reaches a wide flat maximum, where the absorption coefficient reaches  $1.7 \cdot 10^6 \text{ cm}^{-1}$ . In the region of 20–30 eV, there is a smooth decline of  $\mu(E)$  to  $1.0 \cdot 10^6 \text{ cm}^{-1}$ .

Fig. 3, b shows the spectra of the optical functions  $\varepsilon_1(E)$  and  $\varepsilon_2(E)$ . The spectrum  $\varepsilon_2(E)$  is one of the most important optical functions, its structure and shape are determined by the position of critical state density points. In the fundamental absorption region ( $E > 8 \text{ eV}$ ), the spectra are characterized by a number of peaks in the region of 8–16 eV. The lowest-energy local maximum  $\varepsilon_2(E)$  in the CLBO crystal is observed at 9.3 eV, however, in the region

of 8.4–8.6 eV, the shoulder is noted. The second local maximum is located at 11.0–11.7 eV. At the energy above 13.5 eV, there is a sharp rise in  $\varepsilon_2(E)$  with a wide flat maximum in the area of 17–19 eV. In the energy range 20–30 eV, a monotonous decline of the function  $\varepsilon_2(E)$  is observed.

#### 4. Discussion of results

Anticipating the discussion of the experimental results obtained in this paper, we will consider the most important design base data on the electronic structure of CLBO obtained by zone [32,33] and cluster [24,34] methods. Despite the qualitative agreement between most of the calculated results, the question of the contribution of Li and Cs cations to the electronic structure of CLBO in these works remained controversial. For the beginning of the reference on the energy scale, the level of the vertex VB was taken during the discussion.

According to [33], despite the differences in symmetry, the zone structure of CLBO ( $I\bar{4}2d$ ) is qualitatively similar to that of LBO ( $Pna2_1$ ) and consists of three energy regions: 1) quasi-stable levels (below  $-15 \text{ eV}$ ) formed mainly by  $2s$ -states of oxygen atoms with a small contribution of  $6s$ -orbitals Cs; 2) valence band (from  $-9$  to  $0 \text{ eV}$ ), the plane states of which consist mainly of  $2p$ -orbitals of oxygen atoms, but at  $-5.5 \text{ eV}$  in CLBO there is a significant contribution of  $6p$ -orbitals Cs, and the upper part of the VB from  $-3$  to  $0 \text{ eV}$  is formed by  $2p$ -states of oxygen atoms in the absence of hybridization of states B and O; 3) the conduction band (above  $E_g$ ) is formed mainly by the states of hybridized borooxygen orbitals, in which the band calculation revealed an energy interval of about 1 eV, due to the states of Cs cations. Analysis of the total and partial model densities of states indicates [33] that the orbitals of lithium atoms do not contribute to the electronic structure of CLBO; the width of the energy gap decreases during the transition from LBO to CLBO; the expected contribution of  $d$ -orbitals Cs to the states of the bottom of the conduction band is not detected.

In the work [32] the electronic structure of CLBO is calculated by the zone self-consistent method of non-local pseudopotential. The flat nature of the VB states is revealed and a design base estimate of the energy gap from 6.0 to 6.8 eV is obtained.

In the quantum chemical calculations in a cluster model, an essential circumstance is the choice of the simulated fragments, the ambiguity of which may be one of the reasons for the observed discrepancies between the results of various cluster calculations [35].

So, in the calculation of [24], a simulated fragment of the CLBO lattice was used, in which cesium atoms occupied peripheral positions of the cluster. Cluster calculations of the electronic structure of CLBO [24] showed that the Cs cation states contribute approximately 1.6 eV above the bottom of the CB, while the Cs contribution to the VB

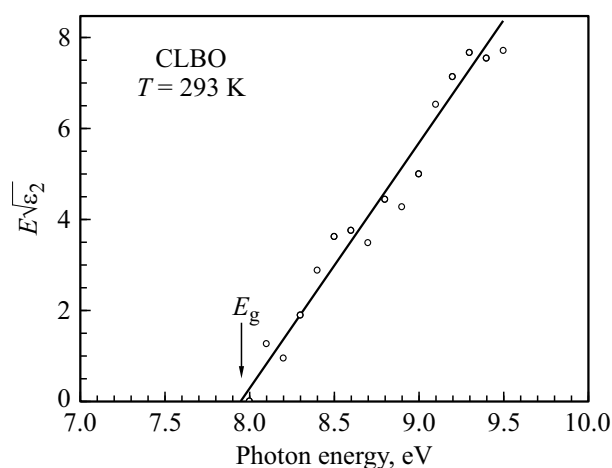


**Figure 4.** The edge of the fundamental absorption of CLBO crystals at  $T = 9.3$  K.

was not detected. The purely covalent nature of the lowest-energy electronic transitions in CLBO is particularly noted, the energy of which should be somewhat lower than those for LBO. This conclusion, however, is in contradiction with experimental data on low-temperature luminescent-optical VUV spectroscopy CLBO [29].

In the work [34], we applied the standard method of self-consistent scattered wave potential (SCS-WP) in a cluster model embedded in a lattice of point charges [36]. The calculated data on the CLBO EO structure were obtained in a cycle of self-consistent calculations of the electronic structure of clusters  $[B_3O_8]^{7-}$  and  $[CsO_4]^{7-}$  with maximum parameterization the crystal as a whole and the crosslinking of the calculation results for two clusters on the spectrum of the same type of oxygen atoms. Analysis of partial model densities of states taking into account photoionization cross sections revealed that the VB CLBO ceiling (from 0 to  $-4$  eV) is formed exclusively by unrelated O  $2p$ -molecular orbitals. The VB region from  $-4$  to  $-11$  eV is formed by Cs  $5p$ -states (peak in the region of  $-6$  eV) and hybridized O  $2p \leftrightarrow B 2s$ , B  $2p$ -molecular orbitals (covalent nature of B–O bonds). The results obtained in the work [34] are consistent with the relative energy position of Cs  $5p$ - and O  $2p$ -states in the CBO crystals [21].

The spectra of  $\epsilon_2(E)$  of the imaginary part of the complex permittivity of CLBO obtained in this work give grounds for a more adequate estimate of  $E_g$ . Indeed, the lowest-energy peak in the  $\epsilon_2(E)$  spectrum is usually compared with the lowest-energy electronic transitions from the top of the valence band to states at the conduction band bottom, so the threshold for interband transitions  $E_g$  can be estimated as the cutoff energy of the low-energy peak  $\epsilon_2(E)$ .

Fig. 4 shows a fragment of the dependence of  $E\sqrt{\epsilon_2}$  on the energy of  $E$ , constructed for the energy region near the absorption edge of the CLBO crystal. It can be seen in Fig. 4 that as the photon energy increases, the background absorption level is replaced by an increasing

absorption represented by a straight line, which shows that the following dependence [37] takes place in this energy range:

$$E^2\epsilon_2 \propto (E - E_g)^2. \quad (3)$$

The observed dependence of  $\epsilon_2$  on the energy in the vicinity of the absorption edge indicates the indirect nature of electronic transitions. Extrapolating a straight line to its intersection with the abscissa axis gives  $E_g = 7.95$  eV. This value can be taken as an experimental estimate of the low-temperature band gap of the CLBO crystal. All the parameters obtained in this work characterizing the CLBO absorption edge are summarized in the table. The table shows that the known estimates of  $E_g$  CLBO for theoretical calculations [24,32] are underestimated by about 1.65–1.7 eV, and for experimental work [29] — are overestimated by 0.55 eV.

The results obtained in this work presented in the table, combined with the calculated data of [24,32–34], allow us to make reasonable judgments about the nature of the fundamental absorption of CLBO in the studied energy range up to 30 eV. Assuming, as a first approximation, that optical transitions occur mainly to the states of the bottom of the conduction band formed by hybridized boroxigen orbitals, the low-temperature optical spectra of CLBO (Fig. 2) should be considered mainly due to electronic transitions from various states of the VB: 1) the spectral region from  $E_g$  to 11 eV is caused by transitions from O  $2p$ -states of the upper part of the VB, for which there is practically no hybridization of boron and oxygen states; 2) the spectral region from 12 to 19 eV is caused by transitions from states of the lower part of the VB, which consist mainly of  $2p$ -orbitals of oxygen atoms with a significant contribution of Cs  $6p$ -orbitals; 3) the spectral range from 23 to 30 eV is due to transitions from quasi-stationary states, which consist mainly of O  $2s$ - and Cs  $6s$ -orbitals.

The low-energy edge of the fundamental absorption of CLBO is caused by optical transitions between the states of the ceiling of the VB (O  $2p$ -states) and the states of the bottom of the CB (hybridized boroxigen orbitals), i.e. transitions within the same anionic group. In this connection, an increase in the fundamental optical absorption of CLBO at a photon energy above  $E_1 = 6.75$  eV should be considered due to exciton excitation in the anionic group, i.e. the edge of the fundamental absorption of CLBO is due to exciton absorption, whereas the threshold of interband transitions  $E_g$  CLBO is located above in the energy domain at 7.95 eV (table). The lowest energy peak in the  $\epsilon_2$  spectrum appears in the region at 8.5–9.5 eV as an „arm“ on the low energy slope of the adjacent peak. Experimentally, this manifests itself in the fact that the LBO optical absorption increases sharply immediately above the fundamental absorption edge, which contrasts markedly with some other borates (for example, BBO, CBO), in which interband transitions at extreme points are symmetry forbidden and fundamental optical absorption becomes observable at energies well above the absorption edge [4].

Parameters of the edge of the fundamental VUV absorption of a CLBO crystal at  $T = 293$  K and an estimate of the low-temperature band gap  $E_g$  at  $T = 10$  K

Parameter	Value	
	Our data	For comparison
$E_1$ , nm	180	180 <sup>1,2</sup>
$E_1$ , eV	6.74	
$E_2$ , eV	6.91	
$E_g$ , eV	7.95	6.25 <sup>3</sup> ; 6.31 <sup>4</sup> ; 8.5 <sup>5</sup>
$E_{\varepsilon_2}$ , eV	8.5–9.5	
$\partial E/\partial T$ , eV/K	$-5.5 \cdot 10^{-4}$	
$\Delta T$ , K	10–293	

Note.  $\lambda_c$  — cutoff wavelength (short-wave boundary of the optical transparency region);  $E_1$  and  $E_2$  — energies at which the absorption coefficient  $k$  is 3 and  $50 \text{ cm}^{-1}$  respectively;  $E_g$  — the band gap;  $E_{\varepsilon_2}$  — the energy position of the maximum of the low-energy peak in the spectrum of  $\varepsilon_2(E)$ ;  $\partial E/\partial T$  — the coefficient of the temperature shift of the absorption edge, for which the reflection spectra measured at the boundaries of the temperature range  $\Delta T$  were used to estimate. Data sources provided for comparison: <sup>1</sup> [11], <sup>2</sup> [13], <sup>3</sup> [32], <sup>4</sup> [24], <sup>5</sup> [29].

A detailed examination of the edge of the fundamental absorption of CLBO at different temperatures indicates that it can be approximated fairly well by the Lorentz curve, and the optical density at the maximum of this absorption band can reach  $10^4 \text{ cm}^{-1}$ . This is quite consistent with the experimentally substantiated assumptions about the existence of exciton-like electronic excitations [29] near the edge of the fundamental absorption of CLBO, which probably overlap with interband transitions. The exciton nature of the CLBO fundamental absorption edge is also consistent with the data for LBO [26,27].

## 5. Conclusion

In this paper, an experimental study of the VUV edge of the fundamental optical absorption of cesium-lithium borate crystals  $\text{CsLiB}_6\text{O}_{10}$  (CLBO) has been performed. Based on the recorded optical transmission, absorption and reflection spectra, a set of parameters characterizing the VUV edge of the fundamental absorption CLBO is obtained: the short-wave boundary of the transparency band (cut-off wavelength); the energy position of the edge of the fundamental absorption, at which the absorption coefficient  $k = 50 \text{ cm}^{-1}$ ; the coefficient of temperature shift absorption edges  $-5.5 \cdot 10^{-4} \text{ eV/K}$ . Based on the low-temperature reflection spectra ( $T = 10 \text{ K}$ ,  $\theta = 17^\circ$ ,  $E = 7\text{--}30 \text{ eV}$ ), the Kramers–Kronig method was used to calculate the spectra optical constants: refraction ( $n$ ) and absorption ( $k$ ) indices, real ( $\varepsilon_1$ ) and imaginary ( $\varepsilon_2$ ) parts of the complex permittivity, and absorption coefficient  $\mu$ . In the spectrum of  $\varepsilon_2(E)$ , the lowest-energy peak caused by electronic transitions from the top of the valence band to the states of the bottom of the conduction band was studied, the threshold of interband transitions  $E_g$  was determined (at  $T = 10 \text{ K}$ ): 7.95 eV. The lowest-energy electronic transition

in lithium borates, which determines the threshold of interband transitions  $E_g$ , occurs between the states of the anionic group that determine the top of the valence band and the bottom of the conduction band. No experimental manifestations of electronic transitions involving lithium or cesium cation states have been identified in the region of the CLBO fundamental absorption edge.

## Acknowledgments

The author is grateful to L.I. Isaenko for providing crystals for research, V.A. Pustovarov — for his interest in the work and assistance in carrying out measurements in the VUV region of the spectrum.

## Conflict of interest

The author declares that he has no conflict of interest.

## References

- [1] V.G. Dmitriev, G.G. Gurzadyan, D.N. Nikogosyan. *Handbook of Nonlinear Optical Crystals* (Berlin, New York, 1999), 413 p.
- [2] A.A. Blistanov. *Krystally kvantocoy i nelineynoi optiki (Crystals of quantum and nonlinear optics)* (MIMiS, M., 2000), 432 p.
- [3] Yu.N. Denisyyuk, A. Andreoni, M.A.S. Potenza. *Opt. Spectrosc.*, **89**, 125 (2000). (in Russian)
- [4] R.H. French, J.W. Ling, F.S. Ohuchi, C.T. Chen. *Phys. Rev B: Cond. Matter*, **44**, 8496 (1991).
- [5] F. Huang, L. Huang. *Appl. Phys. Lett.*, **61**, 1769 (1992).
- [6] C. Chen, Y. Wu, A. Jiang, B. Wu, G. You, R.K. Li, S. Lin. *J. Opt. Soc. Am. B-Opt. Physics*, **6**, 616 (1989).
- [7] Y. Mori, S. Nakajima, A. Miyamoto, M. Inagaki, T. Sasaki, H. Yoshida, S. Nakai. *Proc. SPIE*, **2633**, 299 (1995).
- [8] Y. Mori, S. Nakajima, A. Taguchi, A. Miyamoto, M. Inagaki, T. Sasaki, H. Yoshida, S. Nakai. *AIP Conference Proceedings*, **369**, 998 (1996).
- [9] L. Sharma, H. Daido, Y. Kato, S. Nakai, T. Zhang, Y. Mori, T. Sasaki. *Appl. Phys. Lett.*, **69**, 3812 (1996).
- [10] T. Sasaki, Y. Mori. *Proc. SPIE*, **3244**, 88 (1998).
- [11] T. Sasaki, I. Kuroda, S. Nakajima, S. Watanabe, Y. Mori, S. Nakai. *OSA Proc. on Advanced solid-state lasers*, **24**, 91 (1995).
- [12] Y. Mori, I. Kuroda, S. Nakajima, A. Taguchi, T. Sasaki, S. Nakai. *J. Cryst. Growth*, **156**, 307 (1995).
- [13] Y. Mori, T. Sasaki. *Proc. SPIE*, **2700**, 20 (1996).
- [14] Y. Mori, I. Kuroda, S. Nakajima, T. Sasaki, S. Nakai. *Appl. Phys. Lett.*, **67**, 1818 (1995).
- [15] Y. Mori, I. Kuroda, S. Nakajima, T. Sasaki, S. Nakai. *Jpn. J. Appl. Phys.*, **34**, Pt. 2, L296 (1995).
- [16] T. Sasaki, Y. Mori, I. Kuroda, S. Nakajima, K. Yamaguchi, S. Watanabe. *Acta Crystallogr. C*, **51**, 2222 (1995).
- [17] Y.-N. Xu, W.Y. Ching, R.H. French. *Phys. Rev. B: Cond. Matter*, **48**, 17695 (1993).
- [18] A.B. Sobolev, A.Yu. Kuznetsov, I.N. Ogorodnikov, A.V. Kruzhlov. *FTT*, **36**, 1517 (1994) (in Russian).
- [19] A.Yu. Kuznetsov, A.B. Sobolev, I.N. Ogorodnikov, A.V. Kruzhlov. *Radiat. Eff. Defect. Solid.*, **134**, 69 (1995).

- [20] W.-D. Cheng, J.-T. Chen, J.-S. Huang, Q.-E. Zhang. *J. Chem. Soc. Faraday Trans.*, **92**, 5073 (1996).
- [21] J. Li, C.-G. Duan, Z.-Q. Gu, D.-S. Wang. *Phys. Rev. B: Cond. Matter*, **57**, 6925 (1998).
- [22] A.Yu. Kuznetsov, L.I. Isaenko, A.V. Kruzhalov, I.N. Ogorodnikov, A.B. Sobolev. *FTT*, **41**, 57 (1999). (in Russian).
- [23] W.-D. Cheng, J.-S. Huang, J.-X. Lu. *Phys. Rev. B: Cond. Matter*, **57**, 1527 (1998).
- [24] W.-D. Cheng, J.-T. Chen, Q.-S. Lin, Q.-E. Zhang, J.-X. Lu. *Phys. Rev. B: Cond. Matter*, **60**, 11747 (1999).
- [25] A.N. Vasiliev, V.V. Mikhailin. *Vvedenie v spektroskopiyu dielektrikov (Introduction to dielectric spectroscopy)* (Janus-K, M., 2000), 415 p.
- [26] R.K. Li. *Advanced Photonics Research*, **2**, 2100041 (2021).
- [27] I.N. Ogorodnikov. *FTT*, **64**, 830 (2022). (in Russian).
- [28] L.I. Isaenko, A.P. Yelisseyev. *Chem. Sust. Develop.*, **8**, 213 (2000).
- [29] I.N. Ogorodnikov, V.A. Pustovarov, A.V. Kruzhalov, L.I. Isaenko, M. Kirm, G. Tzimmerer. *FTT*, **42**, 1800 (2000). (in Russian).
- [30] Y.K. Yap, S. Haramura, A. Taguchi, Y. Mori, T. Sasaki. *Opt. Commun.*, **145**, 101 (1998).
- [31] V.V. Sobolev, V.V. Nemoshkalenko. *Metody vychislitel'noy fiziki v teorii tverdogo tela. Elektronnaya struktura poluprovodnikov.* (Naukova dumka, Kiev, 1988), 424 p. (in Russian).
- [32] I.V. Kityk, P. Smok, J. Berdowski, T. Lukasiewicz, A. Majchrowski. *Phys. Lett. A*, **280**, 70 (2001).
- [33] Z. Lin, J. Lin, Z. Wang, C. Chen, M.-H. Lee. *Phys. Rev. B: Cond. Matter*, **62**, 1757 (2000).
- [34] A.Yu. Kuznetsov, A.B. Sobolev, L.I. Isaenko. *Radiation Physics and Chemistry of Condensed Matter (1st Intern. Congress on Radiation Physics, High Current Electronics, and Modification of Materials, V. 1).* (Tomsk, 2000). P. 444.
- [35] V.A. Lobach, A.B. Sobolev, B.V. Shulgin. *Zhurn. strukturnoy khimii*, **27**, 3 (1986). (in Russian).
- [36] A.B. Sobolev, S.M. Yerukhimovich, V.S. Startsev, O.A. Keda. *Zhurn. strukturnoy khimii*, **32**, 17 (1991). (in Russian).
- [37] J. Tauc, R. Grigorovici, A. Vancu. *Phys. Status Solidi B*, **15**, 627 (1966).